Normal-form approach to spatiotemporal pattern formation in globally coupled electrochemical systems

Vladimir García-Morales[1,*] and Katharina Krischer[1,†]
[1]*Physik-Department E19, Technische Universität München, James-Franck-Str. 1, D-85748 Garching, Germany*
(Received 28 July 2008; published 11 November 2008)

We show that the experimental global coupling (GC) of spatially extended electrochemical oscillators is weak close to a supercritical Hopf bifurcation. A center manifold reduction allows then the normal form which comprises the GC and the naturally existing nonlocal (migration) coupling (NLC) to be derived. We show that the interaction between NLC and GC widens the spectrum of coherent structures found in globally coupled oscillatory media and allows for wavelength selection of standing waves, stabilization of phase clusters without breaking phase invariance, and creation of heteroclinic networks connecting families of oscillatory states characterized by different spatial symmetries.

DOI: 10.1103/PhysRevE.78.057201 PACS number(s): 05.45.−a, 47.54.−r, 82.40.Bj

Globally coupled nonlinear oscillators may exhibit complex forms of self-organization in the whole range between incoherence and complete synchronization [1]. In certain surface chemical reactions, the global coupling (GC) is produced through interactions with the gas phase where rapid mixing is realized [2,3]. GC can suppress turbulent behavior with the formation of coherent structures or the stabilization of the uniform oscillation [3].

Compared to purely chemical systems, electrochemical oscillators have the electrostatic double layer potential ϕ_{DL} as an additional dynamical variable. As it was realized during the last decade, GC occurs naturally in these systems, for example, when an external resistance R_e is introduced or when part of the cell resistance R_Ω is compensated, an often applied technique in electrochemical experiments [4–9]. The GC can be either synchronizing (positive GC) or desynchronizing (negative GC), its strength being proportional to the experimentally easily tunable parameter $\gamma \equiv 1 - R_\Omega/(R_e + R_u)$, with $\gamma \in (-\infty, 1]$ [5], where R_u is the uncompensated cell resistance. In this Brief Report, we always consider a one-dimensional working electrode (WE) since the experiments concentrated on this geometry [4,7], although our results can be extended to two dimensions. The GC relates the value of ϕ_{DL} at one point x to the spatial average $\langle \cdots \rangle$ taken over the entire WE $\langle \phi_{\mathrm{DL}} \rangle \equiv \int_{\mathrm{WE}} \phi_{\mathrm{DL}}(x')dx'/L$, where L is the length of the WE. All previous theoretical works concentrated on specific models with a large number of parameters and aimed at describing specific observed patterns. The generic experimental realization of GC in electrochemical systems [4] calls, however, for a general description. In this Brief Report, we tackle this problem establishing the appropriate normal form to deal with globally coupled electrochemical systems in the vicinity of a supercritical Hopf bifurcation (SHB). This is carried out rigorously by means of a center manifold reduction in the vicinity of the SHB. This approach allowed us recently to derive the nonlocal complex Ginzburg-Landau equation (NCGLE) for electrochemical systems [10] in the presence of a nonlocal (migration) coupling (NLC). The NLC depends on the relative arrangement of the WE and the counterelectrode and, thus, its range β can be tuned experimentally [11]. Its nature is essentially different from the one of the GC that we discuss here. The NLC is present in any electrochemical experiment and arises from the distribution of the electrostatic potential in the electrolyte [12]. In contrast, the GC might be introduced by the control of the cell voltage or the current. The repercussions of the NLC and the GC on the dynamical behavior are also very different. In this report, we show that (a) the GC of experimental electrochemical systems scales in a specific way that allows center manifold theory to be applied and that (b) the interaction between NLC and GC enlarges the spectrum of coherent structures reported for globally coupled oscillatory media in several aspects.

The physical dynamics of an electrochemical system under GC is described by the following equations [5,13]:

$$\partial_t \phi_{\mathrm{DL}} = f(\phi_{\mathrm{DL}}, \mathbf{c}) + \frac{\gamma\sigma}{\beta}(\langle \phi_{\mathrm{DL}} \rangle - \phi_{\mathrm{DL}}) + \sigma \int_{\mathrm{WE}} H_\beta(|x - x'|)[\phi_{\mathrm{DL}}(x') - \phi_{\mathrm{DL}}(x)]dx', \quad (1)$$

$$\partial_t \mathbf{c} = \mathbf{g}(\phi_{\mathrm{DL}}, \mathbf{c}), \quad (2)$$

where $\mathbf{c}$ is a vector of chemical species, x and x' are two positions along the 1D WE, σ is the conductivity of the electrolyte, the term proportional to γ/β captures the GC, β controls the range of the NLC, and

$$H_\beta(|x - x'|) = \frac{\pi}{4\beta^2 \sinh^2\left(\frac{\pi(x - x')}{2\beta}\right)} + \frac{\delta(|x - x'|)}{\beta} \quad (3)$$

is the kernel of the NLC term. The local coupling range is obtained with $\beta \to 0$. If we carry out a perturbation approach around the stationary state ϕ_{DL}^0, $\mathbf{c}^0$ in the vicinity of the SHB, to linear order the perturbation of the variable $u \equiv \phi_{\mathrm{DL}} - \phi_{\mathrm{DL}}^0$ scales as $u \approx \varepsilon u_1$ with u_1 being the dominant contribution to the perturbation and ε a small parameter. In electrochemical systems, system length L and coupling range β

*vmorales@ph.tum.de
†krischer@ph.tum.de

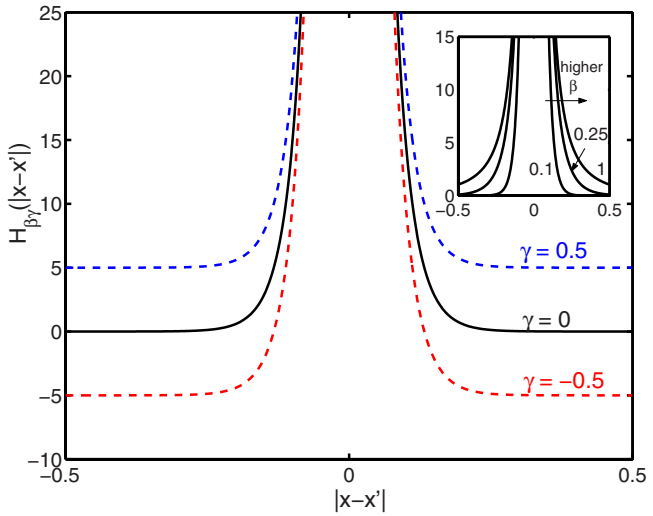

FIG. 1. (Color online) $H_{\beta\gamma}$ calculated from Eq. (6) for $\beta=0.1$ and the values of γ indicated in the figure. Inset: $H_{\beta\gamma}$ for $\gamma=0$ and the values of β indicated in the figure.

scale at criticality as $\tilde{L}=\varepsilon^2 L$ and $\tilde{\beta}=\varepsilon^2\beta$, respectively [10]. Therefore, if we consider the dynamics of the perturbation from Eqs. (1), the GC term scales to dominant order as

$$\frac{\gamma\sigma}{\beta}(\langle u\rangle - u) \approx \varepsilon^3 \frac{\gamma\sigma}{\tilde{\beta}}(\langle u_1\rangle - u_1). \tag{4}$$

This ε^3 dependence of the GC warrants the application of the center manifold theory since the GC is weak at criticality. The GC term balances with the NLC term that enters also in the perturbation expansion at third order [10]. This leads to the extended NCGLE

$$\partial_t W = W - (1+ic_2)|W|^2 W + K(1+ic_1) \times \int_{\mathrm{WE}} H_{\beta\gamma}(|x-x'|)[W(x') - W(x)]dx', \tag{5}$$

where $W(x,t)=|W|e^{i\phi}$ is a complex amplitude with modulus $|W|$ and phase ϕ depending both on space and time t. $H_{\beta\gamma}$, defined by

$$H_{\beta\gamma}(|x-x'|) \equiv H_\beta(|x-x'|) + \frac{\gamma}{\beta L} \tag{6}$$

with $H_\beta(|x-x'|)$ given by Eq. (3), is our new coupling kernel comprising both NLC and GC. c_1 and c_2 are dimensionless parameters that can be calculated from the homogeneous dynamics (their expressions are the same as in Ref. [10]) and K is the conductivity determining the coupling strength. The latter sets the scale of the system and can be set to unity through the rescalings $x\to Kx$ $(L\to KL)$ and $\beta\to K\beta$. However, we take here $L=1$ and, therefore, $K\neq 1$. The kernel of Eq. (6) is represented in Fig. 1 for different values of γ and β. Equation (5) is a key result of this Brief Report.

We explore now the interplay between GC and NLC. We have carried out simulations of Eq. (5) by using a spectral method with 700 Fourier modes, periodic boundary conditions, and an exponential time stepping algorithm [14]. By

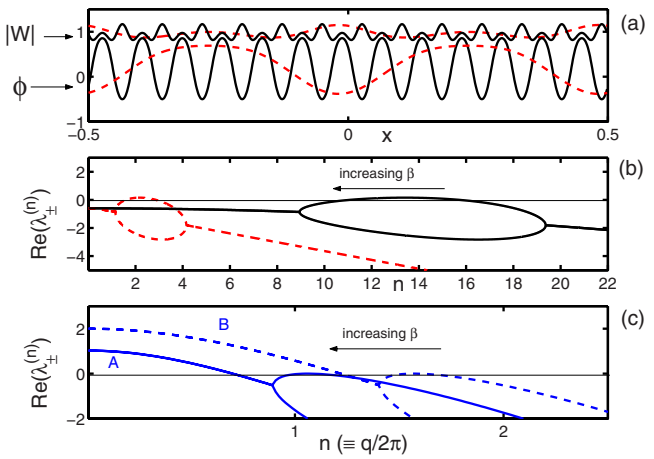

FIG. 2. (Color online) (a) Spatial distribution of $|W|$ and ϕ for $K=0.05$, $c_1=-3.0$, $c_2=1.0$ and $\beta=0.005$, $\gamma=-0.04$ (continuous line) and $\beta=0.5$, $\gamma=-4$ (dashed line). (b) Eigenvalue spectra calculated from Eq. (10) for parameter values corresponding to patterns in (a). (c) Eigenvalue spectra for $K=0.5$, $c_1=-0.5$, $c_2=2.0$, $\gamma=-1.5$, $\beta=0.37$ (A), and $\beta=0.25$ (B) corresponding to patterns (a) and (b) in Fig. 3.

projecting $W=\Sigma_{n=-\infty}^{\infty} W_n e^{i2\pi nx}$ on Eq. (5) and using the Fourier transform of Eq. (6) we obtain for the mode n

$$\dot{W}_n = [1+(1+ic_1)\mathcal{H}^{(n)}]W_n - (1+ic_2)\sum_{j-k+l=n} W_j \bar{W}_k W_l, \tag{7}$$

where the bar denotes complex conjugation and

$$\mathcal{H}^{(n)} \equiv K\left[\frac{1-\gamma(1-\delta_{n0})}{\beta} - 2\pi n \coth(2\pi\beta n)\right] \tag{8}$$

with $\delta_{00}=1$ and $\delta_{n0}=0$ $(n\neq 0)$. Under small, negative GC we observe standing waves. In Fig. 2(a) we show $|W(x)|$ and $\phi(x)$ at a given instant of time for two different standing waves of different periodicity found for two different coupling ranges β and the same γ/β ratio. We see that the larger β is, the longer is the wavelength of the standing waves stabilized by the GC. In Fig. 3 we show spatiotemporal evolutions of $|W|$ and ϕ for higher conductivity $K=0.5$ and decreasing coupling range β from A to C. Ising walls (standing defect lines) are found in the simulations [see Figs. 3(a) and 3(b)] at large coupling range β. Two equal domains oscillate in antiphase (phase clusters) and the $1/2$ spatial translation symmetry is overall broken. Therefore, the general solution for the complex amplitude takes the form $W(x,t)=e^{i\omega_{cl}t}\Sigma_{k=1}^{k_{\max}} w_{2k-1}\sin[2\pi(2k-1)(x-x_0)]$ where x_0 is the position of the wall ω_{cl} and the complex constants w_{2k-1} can be obtained by considering only the odd Fourier numbers $n=2k-1$ in Eq. (7) restricting it to the subspace where the translation symmetry is broken, i.e., $W_{-(2k-1)}=-W_{2k-1}\equiv w_{2k-1}e^{i\omega_{cl}t}/2$. $k_{\max}$ corresponds to the highest wave number active in the pattern. In the simulations we find that the lower β is, the higher $k_{\max}$ is. For high β [as in the pattern in Fig. 3(a)], $k_{\max}=1$. In this case, the solution reads

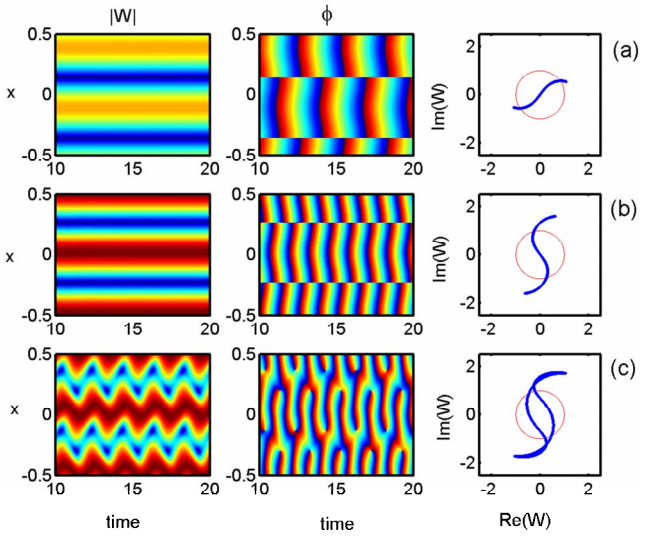

FIG. 3. (Color online) Spatiotemporal evolution $|W|$ (left) and ϕ (middle). Parameter values: $K=0.5$, $\gamma=-1.5$ and $c_1=-0.5$, $c_2=2.0$, $\beta=0.37$ (a), $\beta=0.25$ (b), and $\beta=0.2$ (c). Right: snapshot of W in the complex plane.

$$W(x,t) = 2e^{i\omega_{cl}t+\phi_0}\sqrt{\frac{1}{3}(1+\mathcal{H}^{(1)})}\,\sin[2\pi(x-x_0)] \qquad (9)$$

with $\omega_{cl}=(c_1-c_2)\mathcal{H}^{(1)}-c_2$ and $\mathcal{H}^{(1)}$ given by Eq. (8) with $n=1$. Here ϕ_0 is the initial phase. Equation (9) is accurate and captures all essential features of the phase clusters even when $k_{\max}>1$ [as in Fig. 3(b) where $k_{\max}=4$] since the first Fourier mode always has the strongest contribution to the pattern. Specifically, the frequency of the clusters and the modulus of their amplitude increases with decreasing β, which enters in Eq. (9) through $\mathcal{H}^{(1)}$. This is clearly observed in the simulations in Figs. 3(a) and 3(b) (middle and right columns). These phase clusters were found in experiments with negative GC [4] but a physically meaningful normal form has been lacking for them. For lower β, the walls oscillate [Fig. 3(c)] and in the local coupling limit (here approximately $\beta<0.004$) we are left with turbulence (not shown). This bifurcation to an oscillating wall was also observed in the forced Ginzburg-Landau equation (FCGLE) [15,16]. However, there is a crucial difference between our NCGLE and the FCGLE. The former is gauge invariant, i.e., Eq. (5) remains unchanged after a global transformation $W\to We^{i\eta}$ with η being a real constant number. The FCGLE [15] is not gauge invariant because it contains a term proportional to a power n of the conjugate of the amplitude $\sim\bar{W}^n$.

We can further substantiate all above results from the linear stability analysis of the uniform oscillation. Following the approach in Ref. [10] we find that the latter is stable when

$$\lambda_{\pm}^{(n)} = -(1-\mathcal{H}^{(n)})\left\{1 \pm \sqrt{1-\frac{\mathcal{H}^{(n)}[(1+c_1^2)\mathcal{H}^{(n)}-2\alpha]}{(1-\mathcal{H}^{(n)})^2}}\right\} \qquad (10)$$

is negative for every n and where $\alpha\equiv 1+c_1c_2$. For positive GC, this stability criterion can be written as

$$\frac{\gamma}{\beta} > \frac{-2\alpha}{(1+c_1^2)K} - 2\pi\coth(2\pi\beta) + \frac{1}{\beta}. \qquad (11)$$

In the absence of GC ($\gamma=0$) and in the infinite size limit ($K\to 0$), Eq. (11) becomes the Benjamin-Feir stability criterion [10]. For a positive and sufficiently large value of γ/β we now observe that turbulence can be suppressed in the entire c_1-c_2 plane and arbitrary system size. For negative GC ($\gamma<0$), besides Eq. (11) the following unequality needs also to be satisfied:

$$\frac{\gamma}{\beta} > -\frac{1}{K} - 2\pi\coth(2\pi\beta) + \frac{1}{\beta}. \qquad (12)$$

Standing waves shown in Fig. 2(a) exist when only Eq. (11) is violated with $\gamma<0$. In Fig. 2(b) we plot the real part of the eigenvalues given by Eq. (10) against n for parameter values corresponding to Fig. 2(a). We see that for larger β and constant γ/β the unstable band displaces to longer wavelengths in full consistency with the simulations in Fig. 2(a). When both Eqs. (11) and (12) are violated the phase clusters observed in Fig. 3 are found. The dispersion diagram in this case is shown in Fig. 2(c) for patterns (a) and (b) in Fig 3. The uniform oscillation is destabilized by the wave number $n=1$ that becomes critical, breaking the translation symmetry that leads to the cluster formation. When β is decreased, the eigenvalue spectra are displaced to larger wave numbers, which explains why then $k_{\max}$ increases.

In the limit $\beta\to 0$, Eqs. (5) and (6) become, by defining $\zeta=K\gamma/\beta$ and rescaling $\tau\to\tau/(1-\zeta)$, $x\to x\sqrt{K\beta/3}$ and $W\to W\sqrt{(1-\zeta)}\exp[ic_1\zeta/(\zeta-1)]$, the globally coupled Ginzburg-Landau equation [3]

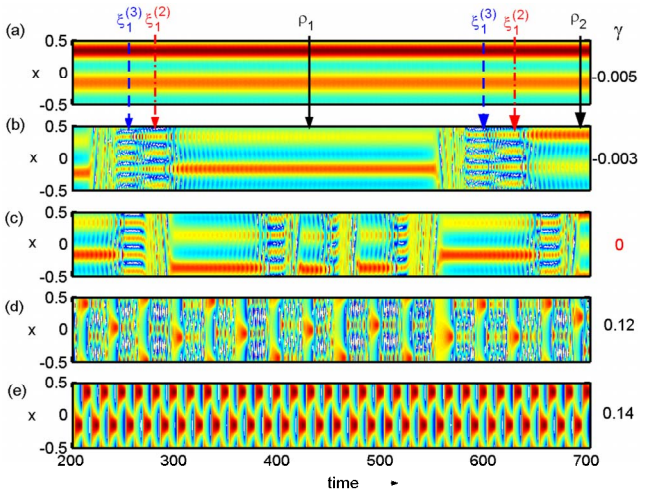

FIG. 4. (Color online) Spatiotemporal evolution $|W|$ for $K=0.005$, $\beta=0.1$, $c_1=-100$, $c_2=0.9$ and the values of γ indicated in the figure. ρ_1 and ρ_2 are limit cycles corresponding to a standing asymmetric pattern. $\xi_j^{(n)}$ is a two-phase cluster state j with $1/n$-translation invariance.

$$\partial_t W = W + (1 + ic_1)\Delta W - (1 + ic_2)|W|^2 W + |\eta| e^{i\chi} \langle W \rangle, \tag{13}$$

where $\eta = \zeta\sqrt{1+c_1^2}/(1-\zeta)$ and $\chi = \tan^{-1} c_1 + [1 - \eta/|\eta|]\pi/2$. It is to be noted that although χ in Ref. [3] played the role of a free parameter, here it takes a fixed specific value and is no longer independent. Equation (13) was *ad hoc* introduced to model globally coupled chemical systems [3]. Here it is the rigorous result for the local coupling limit of the extended NCGLE ($\beta \to 0$), Eq. (5), derived from an electrochemical system. Out of this limit the interplay between GC and NLC leads to extremely rich and complicated behavior, yet highly organized. In Fig. 4 we show spatiotemporal evolutions of $|W|$ for $K=0.005$, $\beta=0.1$, and different values of γ. Already for $\gamma=0$ [Fig. 4(c)] the behavior is complex because of the effect of the NLC. This spatiotemporal pattern is a heteroclinic network [17] connecting families of oscillatory states with different spatial symmetries: Two-phase cluster states $\xi_j^{(n)}$ with translation symmetry $1/n$ ($n=2$ for $\gamma=0$) and limit cycles ρ_j of asymmetric spatial patterns. Most remarkably, for negative GC two phase clusters with $1/3$ translation symmetry are created [see Fig. 4(b)]. For more negative GC a collapse of the network to a ρ_j is observed [Fig. 4(a)]. A positive GC favors transitions within the different states and packs them in coherent structures of lower period and higher contribution of the uniform oscillation W_0 [Fig. 4(d)]. Before the stabilization of the uniform oscillation is achieved [which occurs at $\gamma=0.228$, as calculated from Eq. (11)] a pattern with overall symmetry Z_2 is created [Fig. 4(e)].

In this Brief Report we have established the general model for GC of electrochemical oscillators, Eq. (5). It is to be noted that, despite the presence of four essential parameters c_1, c_2, β, and γ, none of them is free. While the former two ones can be calculated from the homogeneous dynamics of the system, the latter directly address experimental conditions and can be easily tuned in wide parameter ranges. We have shown that the behavior exhibited by Eq. (5) is extremely rich, leading to the stabilization of diverse coherent structures including standing waves, cluster states, and heteroclinic networks.

Financial support from the European Union (project DYNAMO, Contract No. 028669) and the excellence cluster Nanosystems Initiative Munich are gratefully acknowledged.

[1] A. S Mikhailov and K. Showalter, Phys. Rep. **425**, 79 (2006); Y. Kuramoto, *Chemical Oscillations, Waves and Turbulence*, Springer Series in Synergetics (Springer, Berlin, 1984).
[2] M. Kim *et al.*, Science **292**, 1357 (2001); R. Imbihl, Prog. Surf. Sci. **44**, 185 (1993).
[3] G. Veser *et al.*, Phys. Rev. Lett. **71**, 935 (1993); F. Mertens, R. Imbihl, and A. Mikhailov, J. Chem. Phys. **99**, 8668 (1993); **101**, 9903 (1994); M. Falcke, H. Engel, and M. Neufeld, Phys. Rev. E **52**, 763 (1995); M. Falcke and H. Engel, J. Chem. Phys. **101**, 6255 (1994); D. Battogtokh and A. Mikhailov, Physica D **90**, 84 (1996).
[4] K. Krischer, in *Advances in Electrochemical Sciences and Engineering*, edited by D. M. Kolb and R. C. Alkire (Wiley-VCH, Weinheim, 2003), p. 89.
[5] K. Krischer *et al.*, Electrochim. Acta **49**, 103 (2003).
[6] H. Varela *et al.*, Phys. Chem. Chem. Phys. **7**, 2429 (2005); H. Varela, A. Bonnefont, and K. Krischer, ChemPhysChem **4**, 1348 (2003).
[7] R. D. Otterstedt *et al.*, J. Chem. Soc., Faraday Trans. **92**, 2933 (1996); P. Grauel *et al.*, J. Phys. Chem. B **102**, 10264 (1998); J. Christoph *et al.*, J. Chem. Phys. **110**, 8614 (1999); P. Strasser *et al.*, J. Phys. Chem. A **104**, 1854 (2000); J. Lee *et al.*, J. Chem. Phys. **115**, 1485 (2001); P. Grauel, H. Varela, and K. Krischer, Faraday Discuss. **120**, 165 (2001); P. Grauel and K. Krischer, Phys. Chem. Chem. Phys. **3**, 2497 (2001); I. Z. Kiss, W. Wang, and J. L. Hudson, Chaos **12**, 252 (2002); Y. M. Zhai, I. Z. Kiss, and J. L. Hudson, Ind. Eng. Chem. Res. **43**, 315 (2004); S. Fukushima *et al.*, Chem. Phys. Lett. **453**, 35 (2008).
[8] N. Mazouz *et al.*, J. Electrochem. Soc. **145**, 2404 (1998); F. Plenge, H. Varela, and K. Krischer, Phys. Rev. Lett. **94**, 198301 (2005); Phys. Rev. E **72**, 066211 (2005).
[9] F. Plenge, Y. J. Li, and K. Krischer, J. Phys. Chem. B **108**, 14255 (2004).
[10] V. Garcia-Morales and K. Krischer, Phys. Rev. Lett. **100**, 054101 (2008).
[11] H. Varela, C. Beta, A. Bonnefont, and K. Krischer, Phys. Rev. Lett. **94**, 174104 (2005).
[12] V. Garcia-Morales, R. W. Hölzel, and K. Krischer, Phys. Rev. E **78**, 026215 (2008).
[13] J. Christoph, Ph.D. thesis, Free University, Berlin, 1999.
[14] S. M. Cox and P. C. Matthews, J. Comput. Phys. **176**, 430 (2002).
[15] P. Coullet, J. Lega, B. Houchmanzadeh, and J. Lajzerowicz, Phys. Rev. Lett. **65**, 1352 (1990); P. Coullet and K. Emilsson, Physica D **61**, 119 (1992); C. Elphick, A. Hagberg, and E. Meron, Phys. Rev. Lett. **80**, 5007 (1998).
[16] T. Mizuguchi and S. Sasa, Prog. Theor. Phys. **89**, 599 (1993).
[17] P. Ashwin and M. Field, Arch. Ration. Mech. Anal. **148**, 107 (1999); O. Podvigina and P. Ashwin, Physica D **234**, 23 (2007).